Appl. Phys. B (2016) 122:144
DOI 10.1007/s00340-016-6422-z

Applied Physics B
Lasers and Optics

A matrix based on germanium/ormosil system for all-optical applications

Tianxi Gao[1,2] · Wenxiu Que[2] · Yushu Wang[3]

Received: 3 March 2015 / Accepted: 21 April 2016 / Published online: 9 May 2016

Abstract Germania/ormosil hybrid matrix with large third-order nonlinearity is prepared by a low-temperature sol–gel process. Z-scan measurements indicate that the film fabricated from the pure Germania/ormosil hybrid solution shows an excellent third-order nonlinearity at all measured wavelengths. In order to explore its potential to be a functional matrix, a well-investigated organic dopant disperse red 1 (DR1) azoaromatic chromophore is introduced into the Germania/ormosil system. As a comparison, the poly(methyl methacrylate) (PMMA) polymer is employed and doped with the same content of DR1 molecule. Results indicate that by employing Germania/ormosil matrix system, the figure of merit of DR1-doped material at 532 nm can be greatly improved as compared to that of the PMMA/DR1 polymer film and also other published reports. This improvement helps broaden the limited applications of DR1-doped material and make it acceptable for devices fabrication at 532 nm. Results demonstrate that the as-prepared hybrid matrix might be a promising candidate for all-optical applications.

1 Introduction

One of the dreams of scientists is to realize all-optical communication, all-optical transmission, and all-optical computer. In order to make these come true, one of the key is to fabricate workable all-optical processing material [1]. However, at present, mostly optical signal has to be converted to be electrically processed in the electric domain and then be converted back to the optical domain in applications. Such conversions would add unwanted delay and power consumption. In an optical switching, performing information processing solely within optical domain would eliminate the opto-electrical-opto conversion, as well as break the processing limit of the electrical device to be in a sub-picosecond switching period [2]. Light interacts with light by means of a nonlinear material with third-order nonlinearity [3], and the effective index of refraction of the materials will change with the local optical intensity. A device, as Fig. 1 shown, in a Mach–Zehnder geometry used for all-optical signal processing has attracted much attention recently [4–7]. In the absence of any control signal, there is no output signal because of the destructive interference of the input signal; however, when a control signal is applied, the changes in the third-order nonlinear material could alternate the phase of the signal and then lead to constructive interference, thereby enabling all-optical modulation of the input signal. That is how the signal processing is working. Clearly, in such devices, the essential part is the third-order nonlinear cladding, which could directly influence the efficiency of the signal processing.

As a fascinating area for the future generation of data processing, the third-order nonlinear materials have attracted worldwide researchers' attention. However, most related works are focused in the synthetic field [8–11]. The

---

✉ Wenxiu Que
wxque@mail.xjtu.edu.cn

[1] School of Electronic & Control Engineering, Chang'an University, Xi'an 710064, Shaanxi, People's Republic of China

[2] Electronic Materials Research Laboratory, Key Laboratory of the Ministry of Education, International Center for Dielectric Research, Xi'an Jiaotong University, Xi'an 710049, Shaanxi, People's Republic of China

[3] School of Materials Science and Engineering, Georgia Institute of Technology, 500 Tenth Street NW, Atlanta, GA 30318, USA

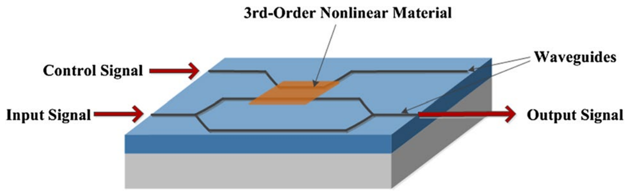

Fig. 1 A device (in a Mach–Zehnder geometry) used for all-optical signal processing

issue is that the third-order nonlinear compounds could not be put into devices in their molecular shape. One of the most common ways is to embed the amazing molecules into proper matrices to fabricate optical functional materials. For instance, as Fig. 1 shows, as a key part of the device, the doped third-order nonlinear cladding is not just involving organic compounds, but also matrices.

As a main kind of matrices, polymers, such as polysiloxanes, polyesters, and polyamides, have been used for doping more than 20 years. Depending on functionalities of the polymer backbones, dyes can be incorporated into the matrices to obtain a good overall mechanical and thermal stability and get a free volume around the dye group [12–14]. Compared with polymers, organically modified silane (ormosil)-based organic–inorganic hybrid system has more rigid inorganic networks and smaller free volume for the doping dye group, which can help freeze the molecules and, as a result, improve the stability of the optical materials and devices. More importantly, some certain kinds of ormosils have excellent nonlinearity themselves and therefore could offer a good foundation of the third-order nonlinearity as a matrix, as well as help the doped material to obtain better nonlinear properties for all-optical applications than polymer does.

Here, we report a matrix with large third-order nonlinearity based on the organic–inorganic hybrid Germania/ormosil system by employing a z-scan technique in different wavelengths, including 532, 800, and 1064 nm. To explore its value to be a compatible matrix for organic compounds to dope, DR1 was chosen as dopant, which has been investigated for more than 20 years, so that there are enough references to be compared with [15–22]. In those previous reports, the figure of merit (*FOM*) of DR1/polymer materials is around 10 at 532 nm. Such values are clearly much higher than the suggested acceptable range *FOM* < 1, which makes DR1 dyes unqualified to be used at 532 nm for all-optical application purpose. In this paper, by doping the same content of DR1 molecules, we compare Germania/ormosils matrix with PMMA, which is one of the most commonly used polymer matrices, to show an improvement taken by our as-prepared matrix.

2 Experimental

Optical hybrid films containing DR1 were prepared by depositing the hybrid solution onto glass slides. Here, germanium isopropoxide ($Ge[OCH(CH_3)_2]_4$) was used as Germania source, and γ-glycidoxypropyltrimethoxysilane (GLYMO, $CH_2OCH\text{-}CH_2O(CH_2)_3Si(OCH_3)_3$) was used as ormosil source. In addition, hydrochloric acid (HCl, 37 wt % in water) was used as catalyst, 2-methoxyethanol ($CH_3OCH_2CH_2OH$) was used to reduce the hydrolysis rate of germanium isopropoxide, ethanol was used as solvent, and deionized water was used for hydrolysis. In particular, the Germania/ormosil organic–inorganic hybrid sols were prepared at room temperature by the sol–gel process. In the preparation, deionized water and hydrochloric acid were added drop by drop, and the molar ratio of HCl/GLYMO was 0.01. The details of the preparation processing of the Germania/ormosil matrix were described in our previous work [23]. To fabricate the DR1-doped Germania/ormosil sols, the commercial DR1 compound in the weight of 1 % of the sol–gel hybrid solution was added into the matrix. One layer of the sol–gel film was spun onto the substrate at 3000 rpm for 30 s by the spin-coating process. The film-coated samples were then heated at 50 °C for about 10 min. As a comparison, the DR1 doped poly (methyl methacrylate) (PMMA) polymer film was also fabricated as follows: PMMA was dissolved in toluene, and thus, a clear solution was obtained with the same viscosity as DR1-doped Germania/ormosil sols has. The DR1 molecule with a weight of 1 % was added into the solution, and then the mixture was stirred for 5–6 h, until a clear and uniform solution was obtained. As Ref. [15] reports, pH has an impact on the absorption spectrum of DR1-doped materials, which could influence the third-order nonlinearity of the materials as well. Therefore, in order to avoid this, we made the PMMA/DR1 solution at the same pH ~ 2.5 as the Germania/ormosil sols was. Afterward, the solution was spun onto the substrate at 3000 rpm for 30 s by the spin-coating process, followed a heat treatment. The parameter of the fabrication process might be fine-turned to make sure the thickness of all the samples are all about 1.55 μm. DR1 dye used in this study was procured from Merck, PMMA from Aldrich, other chemicals, including all the solvents, from Alfa Aesar.

Third-order nonlinear properties of the as-fabricated films were evaluated by a z-scan technique, which can provide a sensitive single-beam technique for measuring both the third-order nonlinear refractive index and the absorption coefficient, as well as their sign. In this paper, we used an optical parametric amplifier (OPA) as the excitation light source. It provides pulses with approximately 30 ps, covering the spectral range from 430 to 2000 nm, with a 10-Hz

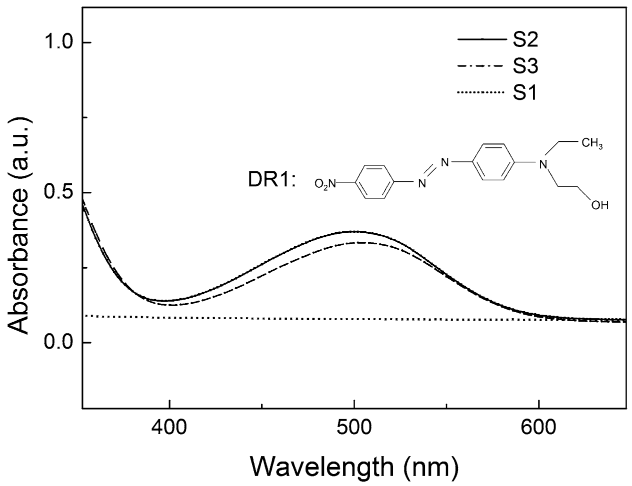

Fig. 2 UV–Vis absorption spectra of the films based on different matrices. S1: pure Germania/ormosil film; S2: DR1-doped Germania/ormosil film; S3: DR1-doped PMMA film

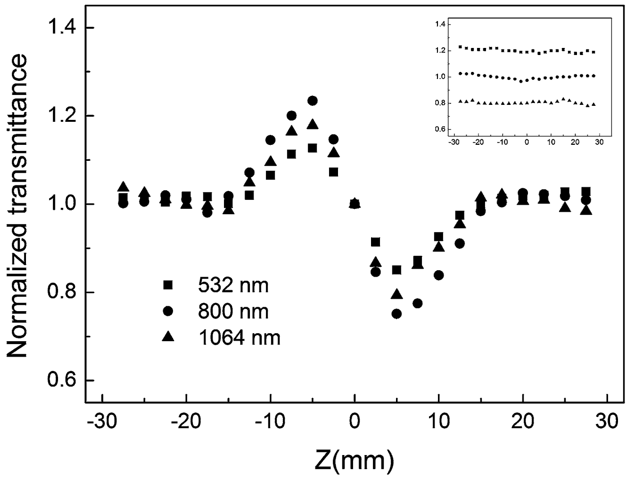

Fig. 3 *Z-scan curves* of the Germania/ormosil hybrid film at different wavelengths

repetition rate. The OPA was pumped by a PL2134B picosecond Nd: YAG laser delivering 12-ps pulses at 532 nm. In order to minimize the error and obtain an average value in z-scan measurement, the incident energy was employed to vary in a lower range of 3.25 ± 0.4 μJ.

3 Results and Discussion

Figure 2 shows the molecular structure of DR1 compound, absorption spectra of the pure Germania/ormosil film, the DR1-doped Germania/ormosil film, and the DR1-doped PMMA film. The DR1-doped films exhibit a high absorption band, located in the visible region, corresponding to the π–π* electronic transitions of the DR1 molecules, while the absorption of the pure Germania/ormosil film is much weaker in the whole visible range. The red color of the doped film is due to the extension of π-electron delocalization in DR1 molecules, which is introduced by a dialkylamino group (π-electron donor) and nitro group (π-electron acceptor). The third-order nonlinear properties of this dye have a wide variety of applications; however, in spite of the superior properties of this dye, its applicability is restricted because it degrades when exposed to intense laser beams. Its opto-chemical, opto-physical, and mechanical stabilities can be improved by being embedded into proper matrix without compromising the nonlinearity of the molecules.

Figure 3 shows the z-scan curves of the pure Germania/ormosil film deposited on glass substrate at 532, 800, and 1064 nm. The main part of the figure is obtained from closed-aperture measurement, while the insert part from the open-aperture measurement. It can be seen that the peaks precede the valleys and perform almost symmetrical configurations in the closed-aperture measurement, while almost no detectible nonlinear absorption could be identified in the open-aperture z-scan measurement at all the three wavelengths. To calculate the third-order nonlinear refractive index and absorption coefficient, n_2 and β can be expressed as follows:

$$n_2 = \lambda \Delta T_{p-v} / \left[0.821\pi (1-S)^{1/4} I_0 L_{eff}\right] \tag{1}$$

$$\beta = 2\Delta T_v / I_0 L_{eff} \tag{2}$$

$$Re\chi^3 esu = 10^{-7} n_2 n_0^2 c / 12\pi^2 \left(cm^2/W\right) \tag{3}$$

$$Im\chi^3 esu = 10^{-7} c\lambda n_0^2 \beta / 96\pi^2 \left(cm^2/W\right) \tag{4}$$

where S, λ, I_0, and L_{eff} are the closed-aperture parameter, wavelength of laser, the power density of laser at the focal plane and the effective thickness of sample, respectively. The value of $\Delta T_{\mathrm{p\text{-}v}}$ can be obtained from the normalized figure obtained by the closed-aperture curve dividing the open-aperture curve, which is the transmittance (T_{p}–T_{v}) difference between the normalized peak and the valley, while the ΔT_{v} can be obtained from the normalized figure obtained by the open-aperture curve. Thus, the third-order nonlinear refractive indices of the Germania/ormosil film generated by different wavelengths were calculated, and their values are at an order of -10^{-10} cm^2/W as Table 1 shows. At 532 nm, the n_2 has a value of $-(5.13 \pm 0.43) \times 10^{-10}$ cm^2/W, and the value of $Re\chi^3$ is also calculated, while almost no detectible nonlinear absorption had been found in all the measured wavelengths.

Table 1 Nonlinear optical parameters of the three samples at 532 nm. S1: pure Germania/ormosil film; S2: DR1-doped Germania/ormosil film; S3: DR1-doped PMMA film

1.	Sample nm	n_2 10^{-10} cm^2/W	β 10^{-5} cm/W	*Re* $\chi^{(3)}10^{-8}$ esu	*Im* $\chi^{(3)}$ 10^{-10} esu	*FOM*
S1	532	$-(5.13 \pm 0.43)$	–	$-(2.92 \pm 0.25)$	–	–
	800	$-(5.64 \pm 0.43)$	–	$-(3.21 \pm 0.25)$	–	–
	1064	$-(4.92 \pm 0.43)$	–	$-(2.80 \pm 0.25)$	–	–
S2	532	$-(7.28 \pm 0.41)$	6.37 ± 0.37	$-(4.15 \pm 0.25)$	2.41 ± 0.14	9.31
S3	532	$-(1.82 \pm 0.54) \times 10^2$	6.45 ± 0.32	$-(1.04 \pm 0.31) \times 10^2$	2.45 ± 0.12	0.38

As reference, CS_2 was also measured at 532 nm, and the obtained n_2 value of CS_2 is $(1.151 \pm 0.19) \times 10^{-11}$ esu, which is in good agreement with the result as reported in the Ref. [24]. To show the potential for the all-optical applications, Stegeman quantified this property by using the figure of merit (*FOM*) as follows: [25]

$$FOM = 2\beta\lambda/n_2 < 1 \tag{5}$$

which means the effect of the nonlinear absorption must be weak as compared to the nonlinear effect, so that could have potential in device applications. For the Germania/ormosil film, clearly, the *FOM* at all the three wavelengths shows excellent values, indicating great potential for all-optical applications. The mechanism for the third-order nonlinear optical response of the sol–gel hybrid matrix mainly originates from the distortion of the electron cloud or the motion of the nuclei. The former has a response time less than 10 fs, while the latter has a relaxation time between 100 fs and 10 ps. In our measurements, the pulse durations give enough time for these two nonlinear optical contributions to be resolved. However, the nonlinear optical contribution of the nuclei is much smaller than that of the electronic part [26]. Therefore, the third-order nonlinear response of the Germania/ormosil hybrid matrix is dominantly produced by the electronic contribution, accompanied with a small nuclear contribution.

To show the advantage by employing the Germania/ormosil matrix system, we take DR1 molecules as dopant to fabricate optical films. The laser we employed in z-scan measurement for DR1-doped films was pulsed at 532 nm, which is near the absorption maxima of DR1. There are two isomers for DR1 molecule, *trans* and *cis*. The *trans–cis* photoisomerization gives rise to large negative third-order nonlinearity in azobenzene. Light frequency near the main absorption resonance causes the azobenzene molecule to be changed from the *trans* isomer to the *cis* isomer. During this process, the distance between the two carbons from which the acceptor and donor groups extend reduces from about 0.9 nm to 0.55 nm. This results in a reduction in the molecules's dipole moment, which reduces the material's polarizability providing a large negative nonlinear refraction. This phenomenon has been investigated over the last two decades. However, such a large nonlinearity accompanies a large nonlinear absorption, which greatly limits its application as an all-optical switching. Our work is to break the limitation by employing the as-prepared matrix in 532 nm. As a comparison, the DR1-doped PMMA film was fabricated to identify the third-order nonlinearity of the pure DR1. To exclude an impact of the PMMA, the blank film sample fabricated from pure PMMA was also measured under the same condition. Results indicate that no detectable signal found from the pure PMMA film; that is, the PMMA matrix gives no contribution to the third-order nonlinearity of the DR1 doped PMMA film. Figure 4 shows the z-scan curves of the 1 % DR1-doped PMMA film, for the main part is the normalized figure obtained by the closed-aperture curve dividing the open-aperture curve, which corresponds to the contribution of the nonlinear refraction, while the insert part is the result of the open-aperture measurement, which represents the contribution of nonlinear absorption only. As have been reported in the Refs. [12, 15, 20], DR1 doped material always presents a negative nonlinear refractive index and a large nonlinear absorption. According to Eqs. (1) and (2), the n_2 is about $-(7.28 \pm 0.41) \times 10^{-10}$ cm^2/W, while the induced nonlinear absorption coefficient β is about $(6.37 \pm 0.37) \times 10^{-5}$ cm/W. The value of $Re\chi^3$ and $Im\chi^3$ is also calculated according to Eqs. (3) and (4) as Table 1 shows. Based on the above results and discussion, among the three main mechanisms of the third-order nonlinearity in azobenzenes: electronic nonlinearity, *trans–cis*

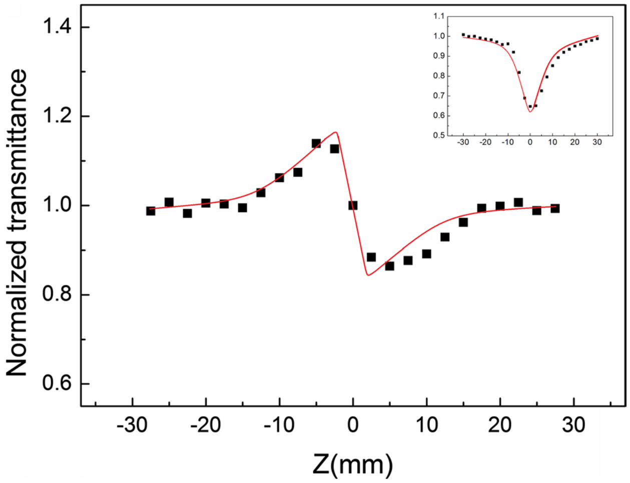

Fig. 4 *Z-scan curves* of the PMMA film doped with 1 % DR1

photoisomerization, and thermal effect, in our present work, the *trans–cis* photoisomerization mechanism should make a main contribution, for the laser pulsed close to the main absorption peak of DR1 molecule. Moreover, considering the strong linear optical absorption of DR1 molecules at 532 nm, thermal nonlinearities could arise from a change in the refractive index with increasing temperature due to the absorption. It should be mentioned that the pulse width and the repetition rate of the laser we employed were controlled low enough to effectively avoid large thermal effect. *FOM* was also calculated, and the value was about 9.31 (>1). Clearly, such value cannot satisfy the requirements for device application enough.

To improve the poor *FOM* of the DR1 doped materials, one method could be considered. It has been proven that the pure Germania/ormosil hybrid matrix system has an excellent third-order nonlinearity. Our previous work [27] demonstrates that 4-hydroxyazobenzene azobenzene compound can be doped into the Germania/ormosil matrix to produce a dense and low absorption and highly transparent organic–inorganic film for photonic application at a low temperature. Here, we introduced it into the third-order nonlinear application as a functional matrix. Figure 5 shows the z-scan curves of the Germania/ormosil film doped with 1 % DR1. It can be observed that the peak precedes the valley in the closed-aperture measurement, demonstrating a negative nonlinear refractive index of the doped film. It also appears as a large nonlinear absorption, which can be found in the deep valley in the open-aperture measurement. According to Eqs. (1) and (2), the third-order nonlinear refractive index n_2 is about $-(1.82 \pm 0.54) \times 10^{-8}$ cm^2/W, while the nonlinear absorption coefficient β is about $(6.45 \pm 0.32) \times 10^{-5}$ cm/W. Furthermore, the figure of merit is also calculated $FOM = 0.38 < 1$, which presents a significant improvement as compared to the PMMA/DR1 system. To make a clear comparison, the nonlinear optical parameters for all the three samples at 532 nm are shown in Table 1. These results indicate that the Germania/ormosil matrix has a good compatibility with the DR1 molecules in the aspect of third-order nonlinear optical response. As compared to the DR1 doped PMMA film, our ormosil/DR1 system gives rise to the third-order nonlinear refractive index, while no obvious extra contribution to the nonlinear absorption. Furthermore, as similar as our PMMA/DR1 reference sample, the *FOM* reported by Refs [20, 28, 29], which embed DR1 into polymers to fabricate nonlinear materials, is all around 10. When compared with those reports, it can be found that the Germania/ormosil matrix presents a great improvement in *FOM* among DR1-doped materials, which change the limited situation for DR1 molecules applied in all-optical applications at 532 nm.

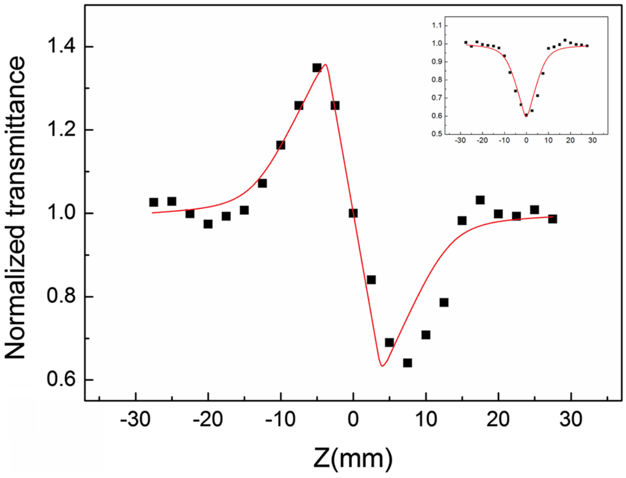

Fig. 5 *Z-scan curves* of the Germania/ormosil hybrid film doped with 1 % DR1

4 Conclusion

We have presented the z-scan measurement results of the Germania/ormosils film at different wavelengths and also DR1-doped films based on different matrices at 532 nm. To effectively avoid large thermal effect, the thickness of all the films were controlled only about 1.55 μm to reduce the thermal accumulation, and a low pulse width and the repetition rate of the laser were also employed during the measurement. Results indicate that the Germania/ormosils film shows large third-order nonlinear refractive indices at an order of 10^{-8} cm^2/W at all measured wavelengths; besides, it also could be used as a functional matrix to help and improve the *FOM* of the DR1-doped films. By employing the Germania/ormosils matrix, the *FOM* of DR1 doped material drops into an acceptable value of 0.38 for device, demonstrating a greatly improvement as compared to 9.31 of PMMA/DR1 film, as well as compared to that of the other reports around 10. All the results indicate that the Germania/ormosil hybrid system could be a promising candidate for all-optical applications as a matrix for compatible dopants.

Acknowledgments This work was supported by the National Natural Science Foundation of China under Grant No. 61078058, by the Research Fund for the Doctoral Program of Higher Education of China under Grant 20120201130004, the Science and Technology Developing Project of Shaanxi Province under Grant No. 2015KW-001, partially by the National Natural Science Foundation of China Major Research Plan on Nanomanufacturing under Grant No. 91323303, and the 111 Project of China (B14040).

Funding This study was funded by National Natural Science Foundation of China under Grant No. 61078058, by the Research Fund for the Doctoral Program of Higher Education of China under Grant 20120201130004, the 111 Project of China (B14040), and the

Science and Technology Developing Project of Shaanxi Province (2015KW-001).

Compliance with ethical standards

Conflict of interest The authors declare that they have no conflict of interest.

References

1. R. Ramaswami, K. Sivarajan, G. Sasaki, *Optical Networks: A Practical Perspective*, 3rd edn. (Morgan Kaufmann Publishers Inc., New York, 2009)
2. J.M. Hale, S. Barlow, H. Kim, S. Mukhopadhyay, J.L. Brédas, J.W. Perry, S.R. Marder, Chem. Mater. **26**, 549–560 (2014)
3. B.E.A. Saleh, M.C. Teich, *Fundamentals of Photonics* chap 19 (John Wiley & Sons Inc., 1991) p. 751
4. C. Koos, P. Vorreau, T. Vallaitis, P. Dumon, W. Bogaerts, R. Baets, B. Esembeson, I. Biaggio, T. Michinobu, F. Diederich, W. Freude, J. Leuthold, Nat. Photonics **3**, 216–219 (2009)
5. J. Leuthold, W. Freude, J.-M. Brosi, R. Baets, P. Dumon, I. Biaggio, M.L. Scimeca, F. Diederich, B. Frank, C. Koos, Proc. IEEE **97**, 1304–1316 (2009)
6. Z. Li, Y. Liu, H. Kim, J.M. Hales, S.-H. Jang, J. Luo, T. Baehr-Jones, M. Hochberg, S.R. Marder, J.W. Perry, A.K.-Y. Jen, Adv. Mater. **24**, 326–330 (2012)
7. M. Hochberg, T. Baehr-Jones, G.X. Wang, M. Shearn, K. Harvard, J.D. Luo, B.Q. Chen, Z.W. Shi, R. Lawson, P. Sullivan, A.K.Y. Jen, L. Dalton, A. Scherer, Nat. Mater. **5**, 703–709 (2006)
8. K. Iliopoulos, I. Guezguez, A.P. Kerasidou, A. El-Ghayoury, D. Branzea, G. Nita, N. Avarvari, H. Belmabrouk, S. Couris, B. Sahraoui, Dyes Pigments **101**, 229–233 (2014)
9. J.M. Hales, J. Matichak, S. Barlow, S. Ohira, K. Yesudas, J.-L. Brédas, J.W. Perry, S.R. Marder, Science **327**, 1485 (2010)
10. K. Kamada, M. Ueda, H. Nagao, K. Tawa, T. Sugino, Y. Shmizu, K. Ohta, J. Phys. Chem. A **104**, 4723–4734 (2000)
11. B. Derkowska, J.C. Mulatier, I. Fuks, B. Sahraoui, X.Nguyen Phu, C. Andraud, J. Opt. Soc. Am. B **18**, 610–616 (2001)
12. S. Yamakawa, K. Hamashima, T. Knoshita, K. Sasaki, Appl. Phys. Lett. **72**, 1562–1564 (1998)
13. T. Kolev, I.V. Kityk, J. Ebothe, B. Sahraoui, Chem. Phys. Lett. **443**, 309–312 (2007)
14. S.F. Fan, D.B. Luo, Optik **122**, 142–144 (2011)
15. V. Rosso, J. Loicq, Y. Renotte, Y. Lion, J. Non-Cryst. Solids **342**, 140–145 (2004)
16. I. Papagiannouli, K. Iliopoulos, D. Gindre, B. Sahraoui, O. Krupka, V. Smokal, A. Kolendo, S. Couris, Chem. Phys. Lett. **554**, 107–112 (2012)
17. R. Rangel-Rojo, S. Yamada, H. Matsuda, D. Yankelevich, Appl. Phys. Lett. **72**, 1021 (1998)
18. L. De Boni, J.J. Rodrigues Jr, D.S. dos Santos Jr, C.H.T.P. Silva, D.T. Balogh, O.N. Oliveira Jr, S.C. Zilio, L. Misoguti, C.R. Mendonc, Chem. Phys. Lett. **361**, 209–213 (2002)
19. J. Li, P. Jiang, C. Wei, J. Shi, Dyes Pigments **78**, 219–224 (2008)
20. L. Misoguti, C.R. Mendonca, S.C. Zilio, Appl. Phys. Lett. **74**, 1531 (1999)
21. L.D. Boni, C. Toro, A.E. Masunov, F.E. Hernández, J. Phys. Chem. A **112**, 3886–3890 (2008)
22. H. El Ouazzani, K. Iliopoulos, M. Pranaitis, O. Krupka, V. Smokal, A. Kolendo, B. Sahraoui, J. Phys. Chem. B **115**, 1944–1949 (2011)
23. W.X. Que, L.L. Wang, T. Chen, Z. Sun, X. Hu, J. Sol-Gel Sci. Techn. **38**, 147–152 (2006)
24. M. Sheik-Bahae, A.A. Said, T.H. Wei, D.J. Hagan, E.W. Van Stryland, IEEE J. Quantum Electron. **26**, 760–769 (1990)
25. G.I. Stegeman, Proc. SPIE **1852**, 75 (1993)
26. J.E. Aber, M.C. Newstein, B.A. Garetz, J. Opt. Soc. Am. B **17**, 120–127 (2000)
27. W.X. Que, C.Y. Jia, M. Sun, L.L. Wang, Z.J. Zhang, Z. Sun, Nanoelectronics Conference (IEEE 2008) pp.176–181
28. R. Rangel-rojo, S. Yamada, H. Matsuda, D. Yankelevich, Appl. Phys. Lett. **72**, 7073 (1998)
29. S. Muto, T. Kubo, Y. Kurokawa, K. Suzuki, Thin Solid Films **322**, 233–237 (1998)